Anatomical distribution of Cancer Stem Cells between Enhancing Nodule and FLAIR hyperintensity in supratentorial Glioblastoma: time to recalibrate the surgical target?

Roberto Altieri (roberto.altieri.87@gmail.com)
Policlinico "G. Rodolico-S. Marco" University Hospital

Giuseppe Broggi
University of Catania

Francesco Certo
Policlinico "G. Rodolico-S. Marco" University Hospital

Daniela Pacella
University of Naples Federico II

Giacomo Cammarata
Policlinico "G. Rodolico-S. Marco" University Hospital

Massimiliano Maione
Policlinico "G. Rodolico-S. Marco" University Hospital

Marco Garozzo
Policlinico "G. Rodolico-S. Marco" University Hospital

Davide Barbagallo
University of Catania

Michele Purrello
University of Catania

Rosario Caltabiano
University of Catania

Gaetano Magro
University of Catania

Giuseppe Barbagallo
Policlinico "G. Rodolico-S. Marco" University Hospital

Research Article

Keywords: glioblastoma, cancer stem cells, FLAIRectomy, 5-ALA, supratotalresection

Posted Date: June 3rd, 2022

DOI: https://doi.org/10.21203/rs.3.rs-1708447/v1

Abstract

It is generally accepted that Glioblastoma (GBM) arise from cancer stem cells (CSC), however, there is little evidence on their anatomical distribution. We investigated the expression and distribution of SOX-2-positive and CD133-positive CSCs both in the enhancing nodule (EN) of GBM and in the FLAIR hyperintensity zones on a surgical, histopathological series of 33 GBMs.The inclusion criterion was the intraoperative sampling of different tumor regions individualized thanks to Neuronavigation and positivity to intraoperative fluorescence with the use of 5-aminolevulinic acid (5-ALA). 33 patients (20 males and 13 females with a mean age at diagnosis of 56 years) met the inclusion criterion. A total of 109 histological samples were evaluated, 52 for ENs and 57 for FLAIR hyperintensity zone. Considering the quantitative distribution of levels of intensity of staining (IS), ES (extent score) and immunoreactivity score (IRS), no difference was found between ENs and FLAIR regions for both the SOX-2 biomarker (respectively, IS p=0.851, ES p=0.561, IRS p=1.000) and the CD133 biomarker (IS p=0.653, ES p=0.409, IRS p=0.881). This evidence suggests to recalibrate the target of surgery for FLAIRECTOMY and 5-ALA could improve the possibility to achieve this goal.

Introduction

It is a matter of fact that the etiology of Glioblastoma (GBM) remains largely unknown. It is generally accepted that GBM arise from cancer stem cells (CSC). Due to their biological features, especially the capability of self-renewal and migratory potential, CSCs might be the starting point of gliomagenesis [1]. It has been widely demonstrated that tumor cells are found beyond the central core of the tumor [2, 3] but there is little evidence about the anatomical distribution of CSCs. Peng et al. recently described, in two autoptic cases of patients affected by GBM [4], a higher expression of CSC immunohistochemical markers at the infiltrating tumor edge with respect to other GBM areas. This evidence suggests that the edge of the tumor is the moving front for tumor progression and invasion and if this was confirmed in vivo and on a larger series, it would lay the foundations for remodulating local treatments on a different target. Based on this assumption, the eradication of CSCs may induce a stable disease-remission, having a potentially curative role on GBM.Many immunohistochemical markers of stem cell differentiation have been studied in different types of cancer [5], but the transcription factor sex-determining region Y-box 2 (SOX-2) and prominin-1, also known as cluster of differentiation 133 (CD133), are the most widely used for brain tumors [6, 7].In this paper we investigated ex vivo the expression and distribution of SOX-2-positive and CD133-positive CSCs both in the central core of GBM (radiologically identified with the Enhancing Nodule -EN- on MRI) and in the peritumoral region (radiologically identified with the FLAIR hyperintensity zone beyond the EN) on a surgical and histopathological series of 15 GBM.

Materials And Methods

We have prospectively collected tissue samples in different tumor areas (see below) and we have then retrospectively retrieved all cases with a histopathologically- and molecularly-proven diagnosis of WHO grade IV IDH-wild type GBM from the Pathology archive of the Department “G.F. Ingrassia” of the

University of Catania, Italy, between January 2020 and December 2021. All these patients were surgically treated at the Neurosurgery Unit of the University-Hospital Policlinico “G. Rodolico-S. Marco”, Catania, Italy. The study protocol was approved by the local ethics committee (CE 165/2015/PO) and all patients had signed a specific informed consent for the study before surgery. The informed consent form for study participation was also approved by the local ethics committee and all signed informed consents were archived in the study files.

The inclusion criterion was pathological proved GBM in patients with an age > 18 y.o. eligible for surgery; intraoperative sampling of different tumor regions (EN and FLAIR) identified thanks to Neuronavigation and intraoperative fluorescence with the use of 5-aminolevulinic acid (5-ALA) (Fig. 1). Pre-operative Gad-T1 and FLAIR sequences were merged with [11C]-methionine Positron Emission Tomography (11[C]-MET PET/CT) on StealthStation S8 (Medtronic Navigation, Louisville, CO, USA) and we took different tissue samples targeting the EN and FLAIR hyperintense areas beyond the tumoral central core identified with Gad-T1 and [11C]-methionine uptake. Only tumor samples with clear 5-ALA fluorescence were selected for the analyses of the different tumor zones. The surgical protocol for resectable tumors was previously detailed [8, 9] and the intraoperative fluorescence was evaluated using a surgical microscope with 400 nm filter (Zeiss; Kinevo®) by 3 trained Neurosurgeons (G.B., F.C., R.A.). The unresectable tumors (deep/eloquent locations, low KPS etc) were biopsied with frameless neuronavigated system (Navigus, Medtronic) and every sample were also evaluated for 5-ALA positivity (Fig. 2).

Of the 58 patients, surgically treated for brain tumor, 33 (20 males and 13 females with a mean age at diagnosis of 56 years) met the inclusion criteria and were included in the study. 22 (66,6%) underwent resection while 11 (33,3%) underwent biopsy. A total of 109 histological samples were evaluated, 52 for EN and 57 for FLAIR hyperintensity zone. The clinico-pathological features of the GBM cases are summarized in Table 1.

Table 1
Clinico-pathological features of the GBM cases

GBM cases	Gender	Mean Age (years)	Anatomic Location	N. of samples from EN	N. of samples from FLAIR
n = 33	Male (*n* = 20) Female (*n* = 13)	56	Temporal L (*n* = 13) Frontal L(n = 9) Parietal L(n = 8) Occipital L (n = 2) Corpus Callosum (n = 1)	52	57
Abbreviations: GBM, glioblastoma; EN, enhancing nodule; L, lobes					

Hematoxylin and eosin (H&E)-stained slides and additional slides stained with numerous immunohistochemical antibodies were available for each case. All the H&E slides were reviewed by three pathologists (G.B., R.C., and G.M.) to confirm the histopathological diagnosis and the correct sampling of the EN and FLAIR regions.

Immunohistochemical analyses were performed on both EN and FLAIR samples, as previously described [10, 11]. Deparaffinized sections were incubated with rabbit polyclonal anti-SOX-2 (ab97959; 1µg/ml; Abcam, Cambridge, UK) and rabbit monoclonal anti-CD133 (ab222782; 0.5 µg/ml; Abcam, Cambridge, UK) for 15 and 30 min at room temperature, respectively. A semiquantitative assessment of the immunohistochemical staining was performed by three pathologists (G.B., R.C. and G.M.) with no access to the clinico-pathological data of the patients, as previously described [12, 13]. SOX-2 and CD133 were considered positive if brown chromogen was observed within the tumor cell nuclei and cytoplasm, respectively.

The intensity of staining (IS) was classified on a 0–3 scale: absent, 0; mild, 1; moderate, 2; strong, 3. Similarly, 5 groups of extent scores (ES; the percentage of stained cells) were found: <5%, 0; 5–30%, 1; 31–50%, 2; 51–75%, 3; >75%, 4.

The immunoreactivity score (IRS), originating from the IS multiplied by the ES, was obtained: the immunohistochemical expressions of SOX-2 and CD133 were considered low if the IRS was ≤ 6, and high if the IRS > 6.

Statistical Analyses

EN and FLAIR levels of IS, ES and IRS for each stem cell marker (SOX-2 and CD133) are described as Median with 95% confidence interval for quantitative data and with frequency and percentage for categorical data. Difference within subjects between EN and FLAIR regions were computed with Wilcoxon signed-rank test for quantitative values, while categorical differences between EN and FLAIR levels were computed with Fisher's exact test. For all analyses, a p-value < 0.05 was considered statistically significant. Analyses were performed using the statistical software R, version 4.0.3.

Results

All samples were fluorescent according to the inclusion criteria, the EN revealed a lava-like fluorescence while FLAIR samples had a faint fluorescence. Immunohistochemical results are summarized in Tables 2,3 and Fig. 3. All histological samples from the EN region showed a proliferation of tumor cells with ovoidal, to elongated, morphology, moderate to severe nuclear atypia, brisk mitotic activity, foci of necrosis and/or microvascular proliferation; all these features were consistent with the diagnosis of WHO grade IV GBM [14, 15]. Similarly, histological samples from FLAIR regions exhibited fragments of brain white matter tissue with focal to diffuse infiltration of GBM cells; neither necrosis nor microvascular proliferation were histologically found within these samples.

Table 2
Difference between frequencies of FLAIR and EN levels ≤ 6 and > 6 for both SOX-2 and CD133 biomarkers

Marker	IRS ≤ 6 EN	IRS > 6 EN	IRS ≤ 6 FLAIR	IRS > 6 FLAIR	P-value
SOX-2	6(18%)	27(82%)	8(24%)	25(76%)	> 0.999
CD133	8(24%)	25(76%)	11(33%)	22(67%)	> 0.999
Abbreviations: IRS, immunoreactivity score					

Table 3
Difference between FLAIR and EN levels for both SOX-2 and CD133 biomarkers.

SOX-2								
IS EN Median [95% CI]	IS FLAIR Median [95% CI]	P-value	ES EN Median [95% CI]	ES FLAIR Median [95% CI]	P-value	IRS EN Median [95% CI]	IRS FLAIR Median [95% CI]	P-value
3 [2–3]	**3** [2–3]	**0.7173**	**4** [3–4]	**3** [3–4]	**0.2023**	**8** [8–9]	**9** [8–9]	**0.91**
CD133								
IS EN Median [95% CI]	IS FLAIR Median [95% CI]	P-value	ES EN Median [95% CI]	ES FLAIR Median [95% CI]	P-value	IRS EN Median [95% CI]	IRS FLAIR Median [95% CI]	P-value
2 [2–3]	**2** [2–3]	**0.8037**	**3** [3–4]	**3** [2–4]	**0.2222**	**8** [8–9]	**8** [4–9]	**0.3944**
Abbreviations: IS, Intensity of staining;; EN, enhancing nodule; ES, Extent score; IRS, Immunoreactivity score								

Among the EN regions, the immunohistochemical expression of SOX-2 was high (IRS > 6) in 27/33 cases (82%) and low (IRS ≤ 6) in 6/33 cases (18%). Among the FLAIR regions, high and low immunoexpression of SOX-2 were found in 25/33 (76%) and in 8/33 (24%) cases, respectively. A discrepancy in SOX-2 levels between EN and FLAIR was observed in only 2/33 cases (6%) with no significant difference between the two regions (p = > 0.999) (Fig. 4A, B) (Table 2).

Similarly, the immunohistochemical expression of CD133 was high (IRS > 6) in 24/33 (73%) and low (IRS ≤ 6) in 9/33 (27%) %) GBM ENs. In addition, high and low CD133 immunoexpression were observed in 22/33 (67%) and 11/33 (33%) GBM FLAIR regions, respectively; for CD133, a discrepancy between EN and FLAIR was seen only in 3/33 cases (9%), with no significant difference between them (p = > 0.999) (Fig. 4C, D) (Table 2).

Considering the quantitative distribution of levels of IS, ES and IRS, no difference was found between the EN and FLAIR regions for both the SOX-2 biomarker (IS p = 0.7173, ES p = 0.2023, IRS p = 0.91) and the CD133 biomarker (IS p = 0.8037, ES p = 0.2222, IRS p = 0.3944) (Table 3).

IS, ES, IRS of each patient are summarized in Supplementary Table.

Discussion

One of the most debated Neuro-oncological issues today is the use of an aggressive resection beyond EN for GBM, this question arose from the evidence that recurrences generally occur in peritumoral areas [16–18]. It has been demonstrated that cellular composition and molecular signatures of the GBM core compared with infiltrative margins are different and many papers described the role of cross-talk between tumoral cells and the tumoral microenvironment in the regulation of tumor growth and progression [19–21].

The first evidence of the key role of CSCs in tumor maintenance, growth and recurrence originated from studies conducted in hematopoietic and solid neoplasms [5]. CSCs are a subpopulation of cells with several capabilities, including self-renewal, multi-cell lineage differentiation and induction of resistance to conventional therapies. As demonstrated in other human neoplasms, CSCs were also isolated in GBMs in 2002 [22, 23]; although their origin is still largely unknown, these cells have been shown to play an initiating role in gliomagenesis, inducing angiogenesis, metastatic spread and resistance to conventional radiotherapic and chemotherapic treatments [6]. Furthermore, CSCs seem to have an increased DNA repair mechanism, through which they tend to easily overcome the cell stress induced by anti-cancer therapy, resulting in shorter resistance and disease recurrence times in GBM patients [24]. Due to the critical role played by CSCs in gliomagenesis, several studies have been carried out to better understand their genetic and immunohistochemical features, as well as their anatomic distribution, in patients affected by malignant gliomas. Based on these assumptions, it has been suggested that, eradicating CSCs, might affect stable, longlasting remission and potentially treat cancer [25, 26].

The detection of proteins that are differentially expressed by CSCs and targetable by immunohistochemistry, represents the best and easiest way to study the expression and distribution of this cell subpopulation [6]. SOX-2 and CD133 are the most used immunomarkers of CSCs in GBM.

The SOX-2 gene, located on chromosome 3q26.3-q27, is part of the SOX family of transcription factors [27]. It encodes a protein that is highly expressed during the development of the central nervous system and downregulated when neural cells start to differentiate; SOX-2 is involved in the regulation of several genes that play key roles in neurogenesis and gliogenesis[7]. In the adult unaffected brain, SOX-2 expression is almost absent and restricted to proliferating cells, neural stem cells and progenitor cells. In brain tumors, SOX-2 expression has been found in glial tumors, such as astrocytomas, oligodendrogliomas and ependymomas, but not in neuronal neoplasms; in particular, a higher histological grade is associated with a higher expression of this protein [7, 28].

CD133, also known as prominin1, is a cell surface transmembrane glycoprotein, originally isolated from murine neuroepithelial cells [29]. It has been demonstrated that CD133-positive tumor cells have a greater tumorinitiating capability and high selfrenewal ability. CD133-positive tumor cells also show more rapid DNA repair than those with no expression of CD133. Assuming the central role of CSCs in the

physiopathology of GBM, they could be a good therapeutical target for local treatment but there is little evidence on their anatomical distribution. Lama et al. demonstrated the presence of CSCs in peritumoral areas of GBM [30]. Angelucci et al. showed that CSCs residing in peritumoral tissue and in central core tumors show different biological behavior. They demonstrated in a samples of 4 patients affected by GBM that the comparison between CSCs of both areas is different in terms of proliferative potential, ultrastructure and expression of stem cell markers, c-Met, MAPK, H19 lncRNA and miR-675-5p, suggesting that CSCs of peritumoral areas are less aggressive than CSCs of the central core [31,32].

Peng et al. [3] studied the different percentage of CSCs on an autoptic series of two patients affected by GBM and described their spatial distribution identifying CSCs with CD133 and SOX-2. They found that the greatest concentration of SCSs were in the peritumoral edge suggesting that the areas beyond the EN are responsible for progression and tumor recurrence [4].

We first compared the concentration of CSCs in the EN and FLAIR hyperintensity zones using the aid of a multimodal intraoperative imaging approach (especially Neuronavigation and a metabolic intraoperative fluorescence tracer) to select the correct samples [33]. We found that 5-ALA correlated with the presence of CSCs. The peritumoral areas, corresponding to the FLAIR hyperintense zone, are populated by CSCs in the absence of necrosis and microvascular proliferation. There are no differences in CSC concentration between EN and FLAIR, which is in agreement with our hypothesis of GBM growth parabola that we previously described with a radiological series. This evidence indeed seems to suggest that gliomatogenesis starts in some specific areas of the brain thanks to a favorable microenvironment. The neural stem cell undergoes transformation in CSC and this population replicates in the corresponding FLAIR areas with a velocity of mean diametric expansion of about 40 mm/years. The continuous accumulation of mutations determines the acquisition of a more malignant property in some areas that acquire a velocity of mean diametric expansion of about 45 mm/year. This is radiologically visible with the appearance of the EN that appears more than 1 year after the first molecular events. Therefore, the discrepancy between the metabolic needs and supply, create the central core necrosis with a deceleration of EN velocity of mean diametric expansion according to the Gompertz curve [34, 35]. In this way, if we surgically treat the EN, the presence of CSCs within the FLAIR zone starts the processes that will lead to the genesis of another EN. This is in agreement with the median free progression survival of 5 months without radiotherapy [36]. At this time there is no evidence about the possibilities to individualize the CSCs with radiomic technologies. Their surgical mapping could open the way to planning local treatment (surgery and radiotherapy) on the new imaging showing the real therapeutical target. Another future perspective could be to find an intraoperative tool (intraoperative fluorescent dye?) to visualize CSCs as well as guiding and maximizing resection.

Conclusion

We have confirmed that 5-ALA can visualize a tumor beyond the classical margins of the EN and we have histologically proved that there are no differences between the concentration of CSCs in FLAIR and EN of GBM. This evidence suggests to recalibrate the target of surgery and radiotherapy in order to achieve a

better local control of the disease. In this way 5-ALA could improve the possibility of achieving a FLAIRECTOMY and, if effected within the functional boundaries, could improve patient outcome. Neuronavigation could have some degree of inaccuracy due to brain shift. Therefore, the sampling of FLAIR tissue versus EN could be theoretically inaccurate. However, the neuronavigation update with intraoperative CT scan [8, 9], surgical experience of trained Neurosurgeons on distinguishing different tissues, the use of 5-ALA besides the number of patients who underwent frameless neuronavigated needle biopsy mitigates this limitation. CD 133 and SOX-2 alone could be disputable as stemness markers but there is a robust literature about the trustworthiness of each marker and we have tested both to enhance their reliability.

Declarations

Ethical approval: The study was conducted in accordance with the Declaration of Helsinki, and approved by the Catania 1 Ethics Committee, Santa Sofia 78 street, Catania, Italy (CE 165/2015/PO).

Consent to participate: Written informed consent has been obtained from the patients to publish this paper if applicable.

Human and Animal Ethics The study was conducted with human biological material in accordance with the Declaration of Helsinki, and approved by the Catania 1 Ethics Committee, Santa Sofia 78 street, Catania, Italy (CE 165/2015/PO).

Consent for publication: Written informed consent has been obtained from the patients to publish this paper if applicable.

Availability of supporting data: the datasets used and/or analysed during the current study are available from the corresponding author on reasonable request.

Competing interests: This research received no external funding. We declare that none of the authors have competing financial or nonfinancial interests.

Authors' Contributions: Study design and manuscript writing: R.A and G.B. Provision of tumor samples: G.B., F.C., R.A. Collection and processing of tumor tissue: D.B., M.P., G.B., R.C., and G.M. Immunohistochemical analyses: G.B., R.C., and G.M. Collection of patient data and clinical information: R.A., F.C., G.C., M.M., M.G. Statistical analysis: D.P. Preparation of figures: G.B. and G.C Contribution to and approval of manuscript: all authors.

Acknowledgments: We thank the Ginetta Ferraguti Association and the Scientific Bureau of the University of Catania for language support.

Supplementary Materials: The following supporting information can be downloaded. Table S1: Immunohistochemical expression of stem cell markers SOX-2 and CD133 in GBM cases.

References

1. Sanai N, Alvarez-Buylla A, Berger MS. Neural Stem Cells and the Origin of Gliomas. New England Journal of Medicine 2005; 353:811–22. https://doi.org/10.1056/NEJMra043666.
2. Stummer W. Mechanisms of tumor-related brain edema. Neurosurgical Focus 2007; 22:1–7. https://doi.org/10.3171/foc.2007.22.5.9.
3. Lin Z-X. Glioma-related edema: new insight into molecular mechanisms and their clinical implications. Chinese Journal of Cancer 2013; 32:49–52. https://doi.org/10.5732/cjc.012.10242.
4. Peng L, Fu J, Wang W, Hofman FM, Chen TC, Chen L. Distribution of cancer stem cells in two human brain gliomas. Oncol Lett 2019; 17:2123–30. https://doi.org/10.3892/ol.2018.9824.
5. Batlle E, Clevers H. Cancer stem cells revisited. Nat Med 2017; 23:1124–34. https://doi.org/10.1038/nm.4409.
6. Ma Q, Long W, Xing C, Chu J, Luo M, Wang HY, et al. Cancer Stem Cells and Immunosuppressive Microenvironment in Glioma. Front Immunol 2018; 9:2924. https://doi.org/10.3389/fimmu.2018.02924.
7. Annovazzi L, Mellai M, Caldera V, Valente G, Schiffer D. SOX2 expression and amplification in gliomas and glioma cell lines. Cancer Genomics Proteomics 2011; 8:139–47.
8. Certo F, Stummer W, Farah JO, Freyschlag C, Visocchi M, Morrone A, et al. Supramarginal resection of glioblastoma: 5-ALA fluorescence, combined intraoperative strategies and correlation with survival. J Neurosurg Sci 2019. https://doi.org/10.23736/S0390-5616.19.04787-8.
9. Certo F, Altieri R, Maione M, Schonauer C, Sortino G, Fiumanò G, et al. FLAIRectomy in Supramarginal Resection of Glioblastoma Correlates With Clinical Outcome and Survival Analysis: A Prospective, Single Institution, Case Series. Oper Neurosurg (Hagerstown) 2020. https://doi.org/10.1093/ons/opaa293.
10. Cammarata FP, Forte GI, Broggi G, Bravatà V, Minafra L, Pisciotta P, et al. Molecular Investigation on a Triple Negative Breast Cancer Xenograft Model Exposed to Proton Beams. Int J Mol Sci 2020;21. https://doi.org/10.3390/ijms21176337.
11. Piombino E, Broggi G, Barbareschi M, Castorina S, Parenti R, Bartoloni G, et al. Wilms' Tumor 1 (WT1): A Novel Immunomarker of Dermatofibrosarcoma Protuberans-An Immunohistochemical Study on a Series of 114 Cases of Bland-Looking Mesenchymal Spindle Cell Lesions of the Dermis/Subcutaneous Tissues. Cancers (Basel) 2021;13. https://doi.org/10.3390/cancers13020252.
12. Broggi G, Ieni A, Russo D, Varricchio S, Puzzo L, Russo A, et al. The Macro-Autophagy-Related Protein Beclin-1 Immunohistochemical Expression Correlates With Tumor Cell Type and Clinical Behavior of Uveal Melanoma. Front Oncol 2020; 10:589849. https://doi.org/10.3389/fonc.2020.589849.
13. Broggi G, Filetti V, Ieni A, Rapisarda V, Ledda C, Vitale E, et al. MacroH2A1 Immunoexpression in Breast Cancer. Front Oncol 2020; 10:1519. https://doi.org/10.3389/fonc.2020.01519.
14. Banan R, Hartmann C. The new WHO 2016 classification of brain tumors-what neurosurgeons need to know. Acta Neurochir (Wien) 2017; 159:403–18. https://doi.org/10.1007/s00701-016-3062-3.

15. Broggi G, Salvatorelli L, Barbagallo D, Certo F, Altieri R, Tirrò E, et al. Diagnostic Utility of the Immunohistochemical Expression of Serine and Arginine Rich Splicing Factor 1 (SRSF1) in the Differential Diagnosis of Adult Gliomas. Cancers (Basel) 2021;13. https://doi.org/10.3390/cancers13092086.
16. Altieri R, Melcarne A, Soffietti R, Rudá R, Franchino F, Pellerino A, et al. Supratotal Resection of Glioblastoma: Is Less More? Surg Technol Int 2019;35.
17. Li YM, Suki D, Hess K, Sawaya R. The influence of maximum safe resection of glioblastoma on survival in 1229 patients: Can we do better than gross-total resection? Journal of Neurosurgery 2016; 124:977–88. https://doi.org/10.3171/2015.5.JNS142087.
18. Mampre D, Ehresman J, Pinilla-Monsalve G, Osorio MAG, Olivi A, Quinones-Hinojosa A, et al. Extending the resection beyond the contrast-enhancement for glioblastoma: feasibility, efficacy, and outcomes. Br J Neurosurg 2018; 32:528–35. https://doi.org/10.1080/02688697.2018.1498450.
19. Hanahan D, Weinberg RA. Hallmarks of cancer: the next generation. Cell 2011; 144:646–74. https://doi.org/10.1016/j.cell.2011.02.013.
20. Altieri R, Barbagallo D, Certo F, Broggi G, Ragusa M, Di Pietro C, et al. Peritumoral Microenvironment in High-Grade Gliomas: From FLAIRectomy to Microglia-Glioma Cross-Talk. Brain Sci 2021;11. https://doi.org/10.3390/brainsci11020200.
21. Barbagallo D, Caponnetto A, Barbagallo C, Battaglia R, Mirabella F, Brex D, et al. The GAUGAA Motif Is Responsible for the Binding between circSMARCA5 and SRSF1 and Related Downstream Effects on Glioblastoma Multiforme Cell Migration and Angiogenic Potential. Int J Mol Sci 2021;22. https://doi.org/10.3390/ijms22041678.
22. Singh SK, Hawkins C, Clarke ID, Squire JA, Bayani J, Hide T, et al. Identification of human brain tumour initiating cells. Nature 2004; 432:396–401. https://doi.org/10.1038/nature03128.
23. Ignatova TN, Kukekov VG, Laywell ED, Suslov ON, Vrionis FD, Steindler DA. Human cortical glial tumors contain neural stem-like cells expressing astroglial and neuronal markers in vitro. Glia 2002; 39:193–206. https://doi.org/10.1002/glia.10094.
24. Huang Z, Cheng L, Guryanova OA, Wu Q, Bao S. Cancer stem cells in glioblastoma–molecular signaling and therapeutic targeting. Protein Cell 2010; 1:638–55. https://doi.org/10.1007/s13238-010-0078-y.
25. Zhu P, Fan Z. Cancer stem cells and tumorigenesis. Biophys Rep 2018; 4:178–88. https://doi.org/10.1007/s41048-018-0062-2.
26. Schmohl JU, Vallera DA. CD133, Selectively Targeting the Root of Cancer. Toxins (Basel) 2016;8. https://doi.org/10.3390/toxins8060165.
27. Scaffidi P, Bianchi ME. Spatially precise DNA bending is an essential activity of the sox2 transcription factor. J Biol Chem 2001; 276:47296–302. https://doi.org/10.1074/jbc.M107619200.
28. Ma Y-H, Mentlein R, Knerlich F, Kruse M-L, Mehdorn HM, Held-Feindt J. Expression of stem cell markers in human astrocytomas of different WHO grades. J Neurooncol 2008; 86:31–45. https://doi.org/10.1007/s11060-007-9439-7.

29. Jang J-W, Song Y, Kim S-H, Kim J, Seo HR. Potential mechanisms of CD133 in cancer stem cells. Life Sci 2017; 184:25–9. https://doi.org/10.1016/j.lfs.2017.07.008.
30. Lama G, Mangiola A, Proietti G, Colabianchi A, Angelucci C, D' Alessio A, et al. Progenitor/Stem Cell Markers in Brain Adjacent to Glioblastoma: GD3 Ganglioside and NG2 Proteoglycan Expression. J Neuropathol Exp Neurol 2016; 75:134–47. https://doi.org/10.1093/jnen/nlv012.
31. Angelucci C, D'Alessio A, Lama G, Binda E, Mangiola A, Vescovi AL, et al. Cancer stem cells from peritumoral tissue of glioblastoma multiforme: the possible missing link between tumor development and progression. Oncotarget 2018; 9:28116–30. https://doi.org/10.18632/oncotarget.25565.
32. D'Alessio A, Proietti G, Sica G, Scicchitano BM. Pathological and Molecular Features of Glioblastoma and Its Peritumoral Tissue. Cancers (Basel) 2019;11. https://doi.org/10.3390/cancers11040469.
33. Barbagallo G, Maione M, Peschillo S, Signorelli F, Visocchi M, Sortino G, et al. Intraoperative Computed Tomography, navigated ultrasound, 5-Amino-Levulinic Acid fluorescence and neuromonitoring in brain tumor surgery: overtreatment or useful tool combination? J Neurosurg Sci 2019. https://doi.org/10.23736/S0390-5616.19.04735-0.
34. Altieri R, Hirono S, Duffau H, Ducati A, Fontanella M, LA Rocca G, et al. Natural history of de novo High Grade Glioma: first description of growth parabola. Journal of Neurosurgical Sciences 2017. https://doi.org/10.23736/S0390-5616.17.04067-X.
35. Altieri R, Certo F, Rocca GL, Melcarne A, Garbossa D, Bianchi A, et al. Radiological evaluation of ex novo high grade glioma: velocity of diametric expansion and acceleration time study. Radiol Oncol 2020; 55:26–34. https://doi.org/10.2478/raon-2020-0071.
36. Stupp R, Mason WP, van den Bent MJ, Weller M, Fisher B, Taphoorn MJB, et al. Radiotherapy plus Concomitant and Adjuvant Temozolomide for Glioblastoma. New England Journal of Medicine 2005; 352:987–96. https://doi.org/10.1056/NEJMoa043330.

Figures

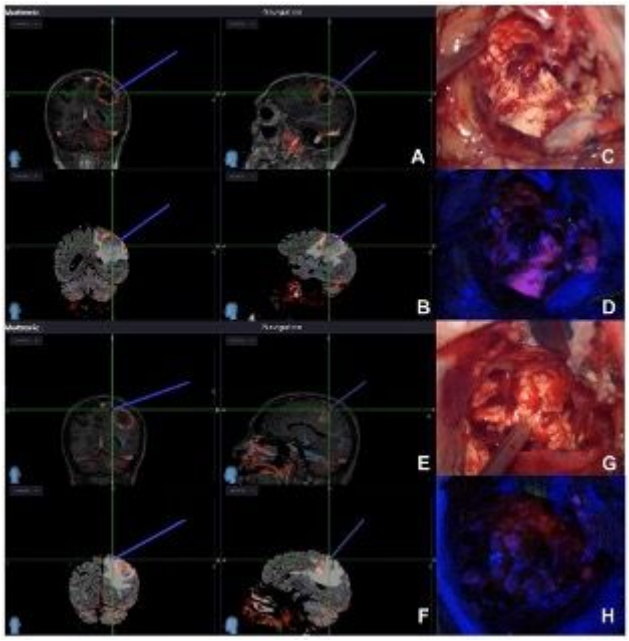

Figure 1

These images show the multimodal intraoperative approach used to select the samples in central core and peritumoral areas. In the first image (A) we can see a screenshot of neuronavigation in which Gad-T1 and FLAIR (B) sequences are merged with [11C]-methionine Positron Emission Tomography (11[C]-MET PET/CT) on StealthStation S8 (Medtronic Navigation, Louisville, CO, USA). The tracer is placed on the edge of the EN zone, confirmed by the overlap with the high uptake area of the PET. The EN is shown under white light (C) and under ultraviolet light filter (D) revealing the presence of lava-like fluorescence. Instead, Gad-T1 (E) and FLAIR (F) sequences merged with 11[C]-MET PET/CT show the tracer placed in the FLAIR hyperintense area beyond the EN. The FLAIR hyperintensity zone is then displayed under white light (G) and under ultraviolet light filter (H) revealing faint fluorescence.

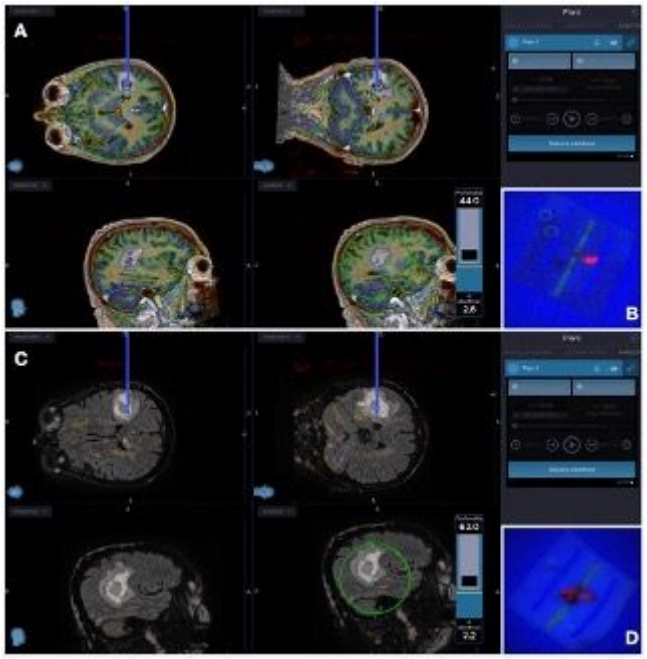

Figure 2

These images show the intraoperative biopsy approach with frameless neuronavigated system (Navigus, Medtronic) used to select the samples in central core and PTA. In the first image (A) we can see T1-Gad sequence merged with 11[C]-MET PET/CT on StealthStation S8. The neuronavigated biopsy needle is placed into the EN, confirmed by the overlap with the high metabolic uptake area. The EN sample is shown under ultraviolet light filter (B) revealing the presence of lava-like fluorescence. Instead, FLAIR sequence merged with 11[C]-MET PET/CT show the neuronavigated biopsy needle placed into the FLAIR hyperintense area beyond the EN/uptake area of the PET. (C) The sample of the FLAIR hyperintensity zone is then displayed under ultraviolet light filter (D) revealing faint fluorescence.

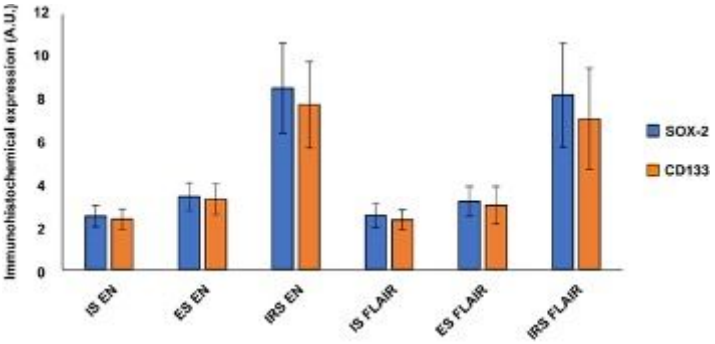

Figure 3

Immunohistochemical expression of stem cell markers SOX-2 and CD133 in GBM cases. Data are represented as mean +/- standard deviation of immunohistochemical expression, reported as arbitrary units (A.U.).

Abbreviations: IS, intensity of staining; ES, extent score; IRS, immunoreactivity score; EN, enhancing nodule.".

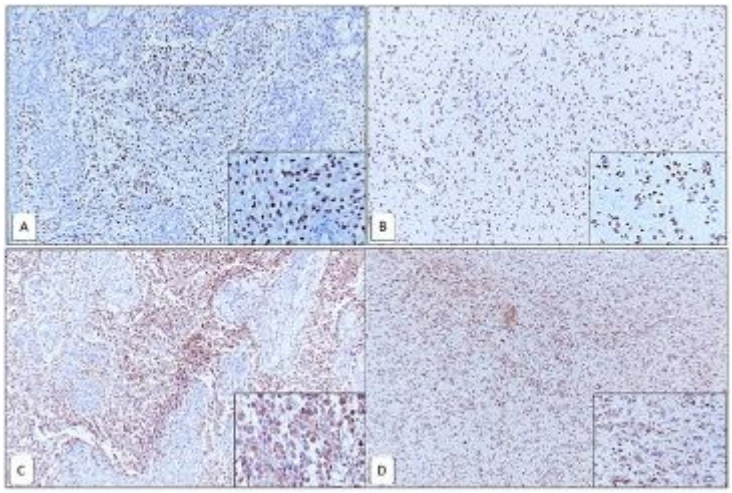

Figure 4

A) Neoplastic cells from EN were diffusely stained with *SOX-2*. Note the diffuse foci of microvascular proliferation and the nuclear immunoreactivity for *SOX-2* (insert). B) High *SOX-2* levels were also observed in the FLAIR regions; diffuse perineuronal satellitosis was seen (insert).

(immunoperoxidase stainings; original magnifications 100x and 200x, inserts). C) High CD133 immunoreactivity in the EN regions. Note the strong cytoplasmic positivity of CD133 (insert). D) Similarly, high CD133 levels were also observed in the FLAIR regions; cancer stem cells, diffusely infiltrating areas of reactive astrogliosis were found (insert). (immunoperoxidase stainings; original magnifications 100x and 200x, inserts)

Supplementary Files

This is a list of supplementary files associated with this preprint. Click to download.

- Supplementaryfile.docx